

Application of the SSA to the Optimal Phase-Swapping Problem in Three-Phase Asymmetric Networks

Aplicación del algoritmo de enjambre de salpas al balance de fases en sistemas trifásicos asimétricos

Antonny Santiago Vargas-Beltrán ^{1a}, Oscar Mauricio Angarita-Santofimio ^{1b}, Oscar Danilo Montoya ^{1c}

¹ Universidad Distrital Francisco José de Caldas, Colombia. Orcid: 0009-0009-7060-6052 ^a, 0009-0005-6711-9756 ^b, 0000-0001-6051-4925 ^c, Email: asvargasb@udistrital.edu.co ^a, omangaritas@udistrital.edu.co ^b, odmontoyag@udistrital.edu.co ^c

Received: 7 March 2023. Accepted: 8 August 2023. Final version: 1 October 2023.

Abstract

This research addresses the optimal phase-balancing problem by applying a master-slave optimization methodology. The master stage defines the load connections per node using a discrete codification, while the slave stage evaluates each load configuration provided by the master stage via a three-phase power flow. For the master stage, the salp swarm algorithm (SSA) was selected, which is an efficient bio-inspired technique to deal with continuous and discrete nonlinear optimization problems. The slave stage employed the matricial backward/forward power flow method for three-phase asymmetric networks. Numerical simulations in IEEE test feeders composed of 8, 25, and 37 nodes confirm the effectiveness of the SSA approach in finding efficient solutions regarding the expected grid power losses after optimal load phase-swapping. Numerical comparisons with the vortex search algorithm, the Chu & Beasley genetic algorithm, and the crow search algorithm demonstrate the effectiveness of the proposed methodology in dealing with the studied problem. All numerical validations were carried out in the MATLAB programming environment.

Keywords: Optimal phase-balancing; Grid power losses; Salp swarm algorithm; Asymmetric distribution systems; Three-phase power flow.

Resumen

Esta investigación aborda el problema del equilibrio de fase óptimo a través de la aplicación de una metodología de optimización maestro-esclavo. La etapa maestra define las conexiones de carga por nodo utilizando una codificación discreta, mientras que la etapa esclava evalúa cada configuración de carga proporcionada por la etapa maestra mediante un flujo de potencia trifásico. Para la etapa maestra, se seleccionó el algoritmo de enjambre de salpas (SSA), una técnica bioinspirada eficiente para lidiar con problemas de optimización no lineal continuos y discretos. La etapa esclava empleó el método matricial de flujo de potencia hacia atrás y hacia adelante para redes trifásicas asimétricas. Las simulaciones numéricas llevadas a cabo en alimentadores de prueba IEEE compuestos por 8, 25 y 37 nodos confirman la eficacia del enfoque SSA para encontrar soluciones eficientes con respecto a las pérdidas de energía esperadas en la red después del cambio de fase de carga óptima. Las comparaciones numéricas realizadas con el algoritmo de búsqueda de vórtices, el algoritmo genético Chu & Beasley y el algoritmo de búsqueda de cuervos

ISSN Printed: 1657 - 4583, ISSN Online: 2145 - 8456.

This work is licensed under a Creative Commons Attribution-NoDerivatives 4.0 License. [CC BY-ND 4.0](https://creativecommons.org/licenses/by-nd/4.0/)



How to cite: A. S. Vargas-Beltrán, O. M. Angarita-Santofimio, O. D. Montoya, "Application of the SSA to the Optimal Phase-Swapping Problem in Three-Phase Asymmetric Networks," *Rev. UIS Ing.*, vol. 22, no. 4, pp. 31-50, 2023, doi: <https://doi.org/10.18273/revuin.v22n4-2023004>

demuestran la eficacia de la metodología propuesta para abordar el problema de estudio. Todas las validaciones numéricas se realizaron en el entorno de programación MATLAB.

Palabras clave: balance óptimo de fases; pérdidas de potencia; algoritmo de enjambre de salpas; redes de distribución asimétricas; flujo de potencia trifásica.

1. Introduction

1.1. General context

The provision and maintenance of electric energy services must consider the set of generation and transmission plants involved, as well as the energy distribution chain and its corresponding energy commercialization [1]. In particular, distribution networks are a component of the electrical system, as they are responsible for reaching the end user via medium transformers that convert medium voltages to low ones [2]. They are made up of feeders, transformer substations, lines, and loads, which are connected by means of nodes [3]. In addition to being the largest part of the power system, distribution grids tend to have longer line lengths than transmission systems [4]. Traditionally, these networks have a radial topology [5], unlike transmission systems, which have a mesh configuration, in association with the reliability required for high-voltage power supplies [6]. These networks regularly have a radial configuration in both rural and suburban areas, and they generally have a primary feeder and lateral branches that, given their topology, have higher energy losses than transmission systems due to heavy loads and voltage collapse [7].

Power flow analysis is used to determine the steady-state operating conditions of distribution networks [8]. The analysis of these grids has been mostly focused on single-phase equivalents. However, this may not be the case for all distribution systems, since some of them cannot be

transformed into this equivalent due to the non-transposition of distribution lines, in addition to the fact that they may have unbalanced loads with delta (Δ) and star (Y) connections [9]. Studies have been recently conducted on this asymmetry, which is due to the nature of the loads and the configuration of the network [10]. This imbalance has negative repercussions on power distribution systems, as there is a current increase in different phases of the system and in the neutral current, as well as over-voltages in the less loaded phases, which will directly increase the power losses and deteriorate the power quality [11]. When comparing these asymmetric networks against symmetric ones, a much higher increase in losses is evidenced in the former [12]. In addition, after measuring the customers' energy consumption, it is necessary to ensure the best billing practices [13]. This

may entail an increase in the bill charged to end users, which can grow to a value of up to 8 % due to energy losses. In the case of the Colombian electricity market, the entity in charge of regulating this energy distribution service is the Energy and Gas Regulatory Commission (CREG) [14].

1.2. Motivation

Energy distribution companies receive economic incentive if they succeed in reducing energy losses, which adds to the high interest in reducing investment costs [15]. Therefore, there is a continuous search for implementing different methodologies in order to reduce energy losses in asymmetric networks. There are long- and short-term approaches that include compensation through shunt devices [16], feeder reconfiguration, and phase balancing, among others [12]. Phase balancing has sparked great interest as one of the most efficient methodologies, as it can provide a higher-quality and lower-cost electric service [17], reduce energy losses, and improve voltage profiles [18], with the advantage of using existing facilities [19]. Therefore, this research work is motivated by the need to propose a new strategy to address the problem of phase balancing in unbalanced three-phase distribution systems.

This is why the proposed methodology defined the active power losses described in Equation (1) as the objective function. This equation correctly models the behavior of an asymmetric three-phase system in a (Y) load configuration. The strategy was able to minimize the active power losses in three asymmetrical test systems, which are detailed in section 4, while decreasing the calculation times with respect to other methodologies applied to phase imbalances in the same networks.

The main drawbacks are outlined in section 2 and pertain to the implementation of functions and constraints with binary, integer, and continuous variables to describe the behavior of different load types in distribution networks. Consequently, the development through matrices that will condense the analyzed IEEE test systems is presented.

1.3. Literature review

To address the problem regarding optimal phase balancing in distribution systems, optimization strategies

of the master-slave type are generally implemented. In these solution methodologies, a combinatorial optimization algorithm is used to define the best set of connections for each of the load nodes, using discrete encoding in the master stage [20]. Subsequently, the power flow method for unbalanced three-phase systems is implemented in the slave stage, with the aim to evaluate each configuration provided by the master stage. In the specialized literature, multiple master-slave algorithms have been proposed to solve the phase balancing problem, some of which are presented below.

The work by [21] proposed a mixed-integer linear programming formulation for determining the optimal phase exchange scheme. The proposed mathematical formulation was evaluated in a 4-node system, and the results showed that it is an effective tool to solve the phase-balancing problem, which can provide better results with respect to the trial-and-error method.

The authors of [22] developed a proposal based on genetic algorithms for solving this optimization problem while improving the phase voltage imbalance, reducing the neutral current in the main transformer, and minimizing energy losses in the system.

In [23], the phase-balancing problem in unbalanced distribution systems was addressed via the ant colony optimization algorithm. The main objective of this work was to reduce the technical losses of the grid, in addition to improving the quality, safety, and reliability of the service. This approach was evaluated in an IEEE 37-node test system located in the state of California, which comprises subway lines, residential loads, and an unbalanced transformer. The results indicate a losses reduction of 9.15 % when compared to the losses of the original system, and they were corroborated by means of the tabu search method, with similar calculation times.

The authors of [24] proposed an optimization methodology that simultaneously considers the phase-balancing problem and the reconfiguration of the network. The methodology applied for reconfiguration was simulated annealing, while the phase-balancing problem was addressed via the ant colony algorithm. To evaluate the proposed methodology, an IEEE test system was used, which had a high imbalance and single- and three-phase loads. The system also had subway lines, a voltage regulator, and a three-phase transformer. The results were compared against those of the separate application of network re-configuration and with a fully balanced system, showing that reconfiguration, when coordinated with other loss reduction methodologies such as phase balancing, can lead to more economical and efficient solutions.

In [25], a multi-objective optimization model was presented in order to address the problem of phase balancing in distribution systems, aiming to minimize the active power losses and the costs associated with the changes made. To solve the mathematical model, a non-dominated sorting genetic algorithm was used. The methodology was evaluated on an IEEE test system with 37 nodes, with the aim to demonstrate its robustness and efficiency, which yielded a set of viable balancing solutions with different cost levels, thus allowing the network operator to choose the most suitable alternative.

The authors of [26] presented a solution to imbalance issues in a three-phase low-voltage network which uses fuzzy evolutionary particle swarm optimization to minimize the system's technical losses, in addition to improving the voltage profiles and the homopolar component associated with the system output. In order to evaluate the proposed method, a system located in a suburban area of the city of San Carlos de Bariloche (Argentina) was employed, which had single-phase and residential loads. Their results were compared to those of the traditional particle swarm algorithm, with good results that were extensible to other test systems.

In [27], the phase equilibrium was solved using a novel method that improves the foreign bacteria algorithm by means of particle swarm optimization through a multi-objective model. This work focused on reducing power losses, the feeder's neutral current, voltage drops, and the cost of phase balancing. The methodology was evaluated in a 72-node system located in Ahwaz (Iran), a network located in a commercial-residential area. The results were compared to those of a genetic algorithm, the immune optimization algorithm, and the foreign bacteria algorithm, yielding a better balance between the network phases, as well as a considerable reduction in power losses and better voltage profiles.

The authors of [28] proposed a method based on the simultaneous reconfiguration and readjustment of distribution networks. A hybrid optimization algorithm called the Nelder-Mead optimizer was used, which was combined with a foreign bacteria algorithm in a multi-objective fuzzy function. To demonstrate its effectiveness, the method was compared against the classical foreign bacteria algorithm, the particle swarm method, a genetic algorithm, and the immune algorithm. Numerical validations were performed on the 123-node IEEE system. The results showed the effectiveness of the method in reducing system costs and balancing network phases in comparison with the classical optimization methods analyzed.

In [29], a differential evolution algorithm was applied as a solution strategy in order to determine the optimal phase balance and size of network conductors. The effectiveness of this method was evaluated on two IEEE systems with 19 and 25 nodes. The results show significant improvements in system power losses and voltage profiles when compared to combinatorial optimization techniques such as genetic algorithms, particle swarm optimization, and the crow search algorithm.

The authors of [30] analyzed the optimal phase-balancing problem using a multi-objective optimization model to minimize energy losses, the neutral conductor current, and the number of network interventions. To solve the mathematical model, a non-dominated sorting genetic algorithm was used. A 4.16 kV test system consisting of two 32-node radial circuits was used. The results of the Pareto front showed a range of options for reducing losses and the neutral current as a function of the number of network interventions.

The study by [31] addressed the energy losses minimization problem in different unbalanced distribution systems. A mixed-integer nonlinear programming mathematical model was used to represent the problem, which was solved using the vortex search optimization algorithm. Three IEEE test systems with 8, 25, and 37 nodes were used, with better results than those obtained using the Chu & Beasley genetic algorithm.

1.4. Contributions and scope

Considering the above, this research makes the following contributions: (i) the application of the salp swarm algorithm (SSA) to the problem regarding optimal phase balancing in three-phase asymmetric distribution networks, using a discrete codification within the framework of a master-slave optimization methodology, whose slave stage uses the matricial backward/forward power flow method to determine the grid power losses; (ii) a complete comparative analysis with different algorithms based on combinatorial methods using the IEEE 8-, 25-, and 37-node test feeders, which allows demonstrating the effectiveness of the proposed approach.

It is worth mentioning that the SSA was selected as the solution methodology in the master stage due to its excellent numerical results in similar optimization problems [32], in addition to the fact that it has not been previously used to deal with the optimal phase-balancing problem.

1.5. Contributions and scope

The remainder of this paper is structured as follows. Section 2 presents the general mixed-integer nonlinear programming (MINLP) model that represents the optimal

phase-swapping problem in three-phase asymmetric distribution networks. Section 3 shows the mathematical formulation necessary for the implementation of the master-slave method, considering the reduction of active power losses in the power system as the objective function, constraints such as active-reactive power balance, an integer variable for phase connection, and the use of a modified SSA with a three-phase power flow matrix method. Section 4 presents the different test scenarios considered, with different node sizes and electrical parameters. Section 5 describes different algorithms from the literature and compares their results with those of the SSA. The final section 6 presents the conclusions and future work proposals derived from this research.

2. Mathematical modeling

The phase-balancing problem in three-phase asymmetric distribution systems can be expressed as an MINLP model with binary decision variables, which, for this study, indicate the connection of the loads in the distribution system [33]. It should be noted that the mathematical model is based on a (Y) load configuration, which typically entails higher losses. Therefore, the IEEE test systems used in Section 4 only used the loads in a (Y) connection. In addition to these decision variables, continuous variables consider the power flow magnitudes and angles, among others. The complete description of the optimal phase-balancing problem in three-phase unbalanced distribution networks is presented below.

2.1. Objective function

The objective function corresponds to the minimization of active power losses in all lines of the system (*i.e.*, P_{loss}). This objective function is defined in Equation (1),

$$\min P_{\text{loss}} = \sum_{m \in \mathcal{N}} \sum_{n \in \mathcal{N}} \sum_{h \in \mathcal{F}} \sum_{i \in \mathcal{F}} Y_{mn}^{hi} V_m^h V_n^i \cos(\delta_m^h - \theta_{mn}^{hi}) \quad (1)$$

where P_{loss} corresponds to the active power function to be minimized; Y_{mn}^{hi} represents the magnitude of the admittance connected between nodes m and n in phases h and i ; V_m^h represents the voltage magnitude at node h ; V_n^i represents the voltage magnitude at node n in phase i ;

δ_m^h is the angle of the voltage of node m in phase h ; and δ_n^i is the angle for the voltage of node n in phase i , where θ_{mn}^{hi} is the angle of the admittance connecting node m in phase h with node n in phase i . It is also important to note that these variables are contained in the sets \mathcal{N} and \mathcal{F} , *i.e.*, \mathcal{N} represents the set containing all the nodes and \mathcal{F} , represents the set containing all the phases of the system.

2.2. Set of constraints

The set of constraints associated with a phase imbalance problem in three-phase distribution systems is given by the active and reactive power balance equations, the voltage regulation limits, and the characteristics associated with the connection of the loads at each node of the system [34]. The set of constraints related to the phase-balancing problem in three-phase systems is presented in Equations (2)–(6).

$$P_m^{sh} - \sum_{i \in \mathcal{F}} x_m^{hi} P_m^{di} = V_m^h \sum_{n \in \mathcal{N}} \sum_{i \in \mathcal{F}} Y_{mn}^{hi} V_n^i \cos(\delta_m^h - \delta_n^i - \theta_{mn}^{hi}) \quad \left\{ \begin{array}{l} \forall h \in \mathcal{F} \\ \forall m \in \mathcal{N} \end{array} \right\} \quad (2)$$

$$Q_m^{sh} - \sum_{i \in \mathcal{F}} x_m^{hi} Q_m^{di} = V_m^h \sum_{n \in \mathcal{N}} \sum_{i \in \mathcal{F}} Y_{mn}^{hi} V_n^i \sin(\delta_m^h - \delta_n^i - \theta_{mn}^{hi}) \quad \left\{ \begin{array}{l} \forall h \in \mathcal{F} \\ \forall m \in \mathcal{N} \end{array} \right\} \quad (3)$$

$$\sum_{i \in \mathcal{F}} x_m^{hi} = 1, \quad \left\{ \forall h \in \mathcal{F}, \forall m \in \mathcal{N} \right\} \quad (4)$$

$$\sum_{h \in \mathcal{F}} x_m^{hi} = 1, \quad \left\{ \forall i \in \mathcal{F}, \forall m \in \mathcal{N} \right\} \quad (5)$$

$$V_{min} \leq V_m^h \leq V_{max}, \quad \left\{ \forall h \in \mathcal{F}, \forall m \in \mathcal{N} \right\} \quad (6)$$

where P_m^{sh} is the variable associated with the active power produced by generator s connected to node m in phase h . Moreover, Q_m^{sh} is the variable associated with the reactive power produced in generator s connected to node m in phase h . The power demanded at node m in phase i is represented by P_m^{di} . The reactive power required at node m in phase i is denoted by Q_m^{di} . x_m^{hi} is a binary variable in charge of the connection demanded at node m in phases h and i . In addition, V_{min} and V_{max} correspond to the voltage regulation limits at the system

nodes. On the other hand, the binary decision variable x_m^{hi} has six possible connection combinations at the demand nodes, as shown in Table 1. It is important not to make changes in the phase sequence of rotating electrical machines in distribution systems, as undesired operation by reverse rotation may occur [35] (see Figure 1).

Table 1. Possible connection types in three-phase distribution system loads

No.	Connection	Sequence
1	ABC	
2	BCA	No change
3	CAB	
4	ACB	
5	CBA	Change
6	BAC	

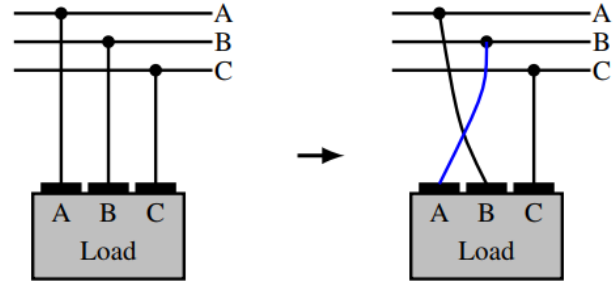


Figure 1. Example of an ABC-BAC connection change in a demand node.

A detailed description of the mathematical model (1)–(8) is presented below.

- i. The objective function (1) represents the minimization of active power losses in the distribution system. Note that it is a nonlinear and non-convex function of the system voltage variables and their angles, and it depends on the physical parameters of the network, *i.e.*, the nodal admittances.
- ii. Equations (2)–(3) model the active and reactive power balance of each node, which corresponds to nonlinear, non-convex constraints due to the presence of products between variables as well as trigonometric functions.
- iii. Equations (4)–(5) model the possible connections of each node, changing the power demanded by each phase according to the different reported combinations Table 1. These two equality constraints ensure that the loads associated with the demand are limited to being connected to one of the six aforementioned possibilities.

- iv. Equation (6) expresses the voltage limits assigned for each node according to the regulatory policy applicable to medium-voltage distribution systems.

Remark 1. Given the nonlinear and non-convex structure of the optimization model (1)–(6) and the large dimension of the solution space, which increases exponentially with the number of nodes in the distribution grid, efficient optimization methods are required to find solutions in reasonable times via a master-slave optimizer connection. The master stage is typically defined as a combinatorial optimization method (i.e., the SSA approach in this study), combined with an efficient three-phase power flow approach in the slave stage. Note that the slave stage in this research is the matricial backward/forward power flow method.

3. Proposed solution methodology

This work proposes a master-slave optimization method based on the combination of the SSA approach and the matricial backward/forward power flow approach to solve the exact optimization model (1)–(6). In the master stage, the SSA approach defines the set of load connections per node using a discrete codification with numbers between 1 and 6 (Table 1). Each combination of load connections provided by the SSA approach is evaluated in the slave stage through the matricial backward/forward power flow, which is entrusted with determining the grid power losses of each solution generated by the SSA approach in order to guide its exploration and exploitation of the solution space. The main details of both stages are presented below.

3.1. Master stage: salp swarm algorithm

The SSA is a heuristic technique for solving single-objective optimization problems, which is based on the behavior of a string of salps while navigating and feeding in the ocean [36]. Salps are similar to jellyfish because of their gelatinous body and the way in which they propel themselves to move [37]. A salp chain seeks to move towards the best food source. Given that this source is continuously changing, the objective of this chain is to explore and exploit the solution space to find a better solution [38]. Salp swarms are among the largest in the world, as their movement and feeding are quite efficient [39]. The main characteristics of the SSA approach used for solving optimization problems are presented below.

3.1.1. Initial population

Like other combinatorial optimization methods, the SSA is an optimization strategy that evolves through populations (groups of solutions to the optimization problem under analysis). Therefore, in a multidimensional space n where a swarm of m salps moves in search of better food sources, each salp in the matrix represents a possible solution, with n being the number of search variables [40]. In each iteration, the position of the salps shows the best food source according to their previous experience. Salps move through the foraging space and adjust their positions depending on the best individual and collective food sources. The salp with the best individual food source is the leader and guides the swarm to better food sources. The shape of the initial population is presented in Equation (7) [41].

$$\mathbf{X} = \begin{bmatrix} x_{11} & x_{12} & \cdots & x_{1n} \\ x_{21} & x_{22} & \cdots & x_{2n} \\ \vdots & \vdots & \ddots & \vdots \\ x_{m1} & x_{m2} & \cdots & x_{mn} \end{bmatrix} \quad (7)$$

where the matrix \mathbf{X} corresponds to the initial population, x_{mj} represents the load connection at the connected node n , and m denotes the individual to which this solution belongs. The initial population requires random numbers corresponding to the solution space, which can be obtained via Equation (8).

$$x_{ij} = \text{round} \left(x_i^{\min} + r_a (x_i^{\max} - x_i^{\min}) \right), \begin{cases} \forall i = 1, 2, \dots, m \\ \forall j = 1, 2, \dots, n \end{cases} \quad (8)$$

where ij represents the row i and column j within the initial population matrix, and r_a is a random value with a uniform distribution between 0 and 1. The limits of the values that it can take in the solution space are contained in x_i^{\min} and x_i^{\max} , which, for the case under study, depend on the different combinations in Table 1.

3.1.2. Evolution criterion

In SSA modeling, a leader must help the salps in the swarm to relocate in order to improve the group's feeding opportunities. This, by having the followers work as a chain that connects to the leader directly or indirectly. This methodology is used in different forms of swarm optimization [42]. According to the evolution criterion, each of the individuals relevant to the population must first be evaluated in the objective function, with the purpose of establishing the best one (x_{best}^t ; note that the

evaluation of the objective function is carried out, in the slave stage, through the three-phase power flow solution), thus finding new possible individuals, as expressed in Equation (9).

$$x_i^{t+1} = \begin{cases} x_{\text{best}}^t + r_1 \left((x^{\text{max}} - x^{\text{min}}) r_2 + x^{\text{min}} \right) & r_3 \geq 0.5 \\ x_{\text{best}}^t - r_1 \left((x^{\text{max}} - x^{\text{min}}) r_2 + x^{\text{min}} \right) & r_3 < 0.5 \end{cases} \quad (9)$$

where x_i^t is the solution i contained in the population, and r_2 and r_3 are random numbers with a uniform distribution which determine the step size or whether it should tend to a limit of the solution space for the next position. As per Equation (9), the updating of the leader depends directly on the position of the food source. Note that r_1 is a coefficient that decreases with every iteration and is aimed at the exploration and exploitation of the solution space. This coefficient is given by Equation (10).

$$r_1 = 2e^{-\left(\frac{Al}{L}\right)} \quad (10)$$

where L represents the maximum number of iterations and l corresponds to the current iteration's value. Note that Newton's law of motion, defined in Equation (11), is used to update the followers' position.

$$x_i^{t+1} = \frac{1}{2} (x_i^{t+1} + x_i^t) \quad (11)$$

Remark 2. Each new individual solution x_i^{t+1} is reviewed to ensure that the lower and upper bounds allowed for the nodal connections at each node are maintained within a feasible solution region in accordance with the information in Table 1; otherwise, the individual solution x_i^{t+1} must be corrected before its evaluation in the slave stage.

3.2. Slave stage: matricial backward/forward power flow method

In the slave stage, the three-phase power flow obtains the active power losses via the *iterative sweep method* [43]. This method iteratively applies Kirchhoff's laws with a backward current sweep and a forward voltage sweep until the desired convergence is reached [44]. To formalize the power flow problem for three-phase systems into a matrix, a branch-node incidence matrix is used, which represents the network's topology and

$$\mathbf{A}_{ni,mh} = \begin{cases} +1, & \text{if the current of branch } n \text{ in phase } i \text{ leaves from node } m \text{ in phase } h \\ -1, & \text{if the current of branch } n \text{ in phase } i \text{ arrives at node } m \text{ in phase } h \\ 0, & \text{if branch } n \text{ in phase } i \text{ is not connected to node } m \text{ in phase } h \end{cases} \quad (12)$$

relates the nodes to the branches of the system [31]. To illustrate the mathematical formulation of the power flow problem in three-phase systems, consider the system presented in Figure 2 and the information regarding its distribution lines in Table 2.

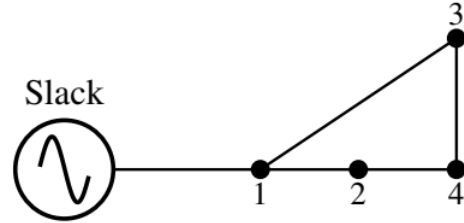


Figure 2. 4-node meshed test feeder.

Table 2. Electrical connection between nodes in a 4-node test feeder

Branch n	Sending node m	Receiving node k
1	1	2
2	1	3
3	2	4
4	3	4

Now, considering this electrical network, in which the direction of the currents in the lines (branches) is randomly defined (Figure 2), the components of the three-phase branch-node incidence matrix $\mathbf{A}_{ni,mh}$ can be obtained using Equation (12), where m corresponds to the sending node, k to the receiving node, n to the branch, and i and h to the phases of the system.

By applying Equation (12) to the example system in Figure 2, the three-phase branch-node incidence matrix shown in (13) is obtained. Note that the branches (rows) have been ordered by phase, according to Table 2, and the columns (nodes) are presented in ascending order, also by phase.

Note that the branch-node incidence matrix in (13) can be compactly represented by two sub-matrices, as shown in (14).

$$\mathbf{A}_{3\phi} = [\mathbf{A}_{s3\phi} \quad \mathbf{A}_{d3\phi}], \quad (14)$$

with \mathbf{A}_{s3phi} being the branch-node incidence matrix, \mathbf{A}_{s3phi} a rectangular matrix relating the branches to the substation node, and \mathbf{A}_{d3phi} a matrix relating the branches to the demand nodes.

On the other hand, if the voltage drop in each branch is determined as the voltage difference between its ending and receiving nodes for each phase, Equation (15) is obtained.

$$\begin{aligned}
E_{1a} &= V_{1a} - V_{2a} \\
E_{1b} &= V_{1b} - V_{2b} \\
E_{1c} &= V_{1c} - V_{2c} \\
E_{2a} &= V_{1a} - V_{3a} \\
E_{2b} &= V_{1b} - V_{3b} \\
E_{2c} &= V_{1c} - V_{3c} \\
E_{3a} &= V_{2a} - V_{4a}' \\
E_{3b} &= V_{2b} - V_{4b} \\
E_{3c} &= V_{2c} - V_{4c} \\
E_{4a} &= V_{3a} - V_{4a} \\
E_{4b} &= V_{3b} - V_{4b} \\
E_{4c} &= V_{3c} - V_{4c}
\end{aligned} \tag{15}$$

which can be rewritten in matrix form, as shown in (16). According to Equation (17), this results in an equivalent compact form.

$$\mathbf{E}_{L3\phi} = \mathbf{A}_{3\phi} \mathbf{V}_{3\phi} \tag{17}$$

where $\mathbf{E}_{L3\phi}$ represents the vector with all voltage drops ordered by branch and phase, and $\mathbf{V}_{3\phi}$ is the vector with all nodal voltages ordered by node and phase. Note that (17) can be written in terms of both generation and

demand, as shown in (18).

$$\mathbf{E}_{L3\phi} = \mathbf{A}_{s3\phi} \mathbf{V}_{s3\phi} + \mathbf{A}_{d3\phi} \mathbf{V}_{d3\phi} \tag{18}$$

On the other hand, if Kirchhoff's first law is applied to each node of the system, the following set of current equations is obtained, which relate the currents of the branches to the net currents injected at the nodes.

Note that the set of equations (19) can be rewritten in matrix form, as presented in (20), which, in turn, can be compacted as (21).

$$\begin{aligned}
I_{1a} &= J_{1a} + J_{2a} \\
I_{1b} &= J_{1b} + J_{2b} \\
I_{1c} &= J_{1c} + J_{2c} \\
I_{2a} &= -J_{1a} + J_{3a} \\
I_{2b} &= -J_{1b} + J_{3b} \\
I_{2c} &= -J_{1c} + J_{3c} \\
I_{3a} &= -J_{2a} + J_{4a} + J_{5a} \\
I_{3b} &= -J_{2b} + J_{4b} + J_{5b} \\
I_{3c} &= -J_{2c} + J_{4c} + J_{5c} \\
I_{4a} &= -J_{3a} - J_{4a} + J_{6a} \\
I_{4b} &= -J_{3b} - J_{4b} + J_{6b} \\
I_{4c} &= -J_{3c} - J_{4c} + J_{6c}
\end{aligned} \tag{19}$$

$$\mathbf{A}_{ni,mh} = \begin{bmatrix} 1 & 0 & 0 & \vdots & -1 & 0 & 0 & 0 & 0 & 0 & 0 & 0 & 0 \\ 0 & 1 & 0 & \vdots & 0 & -1 & 0 & 0 & 0 & 0 & 0 & 0 & 0 \\ 0 & 0 & 1 & \vdots & 0 & 0 & -1 & 0 & 0 & 0 & 0 & 0 & 0 \\ 1 & 0 & 0 & \vdots & 0 & 0 & 0 & -1 & 0 & 0 & 0 & 0 & 0 \\ 0 & 1 & 0 & \vdots & 0 & 0 & 0 & 0 & -1 & 0 & 0 & 0 & 0 \\ 0 & 0 & 1 & \vdots & 0 & 0 & 0 & 0 & 0 & -1 & 0 & 0 & 0 \\ 0 & 0 & 0 & \vdots & 1 & 0 & 0 & 0 & 0 & 0 & -1 & 0 & 0 \\ 0 & 0 & 0 & \vdots & 0 & 1 & 0 & 0 & 0 & 0 & 0 & -1 & 0 \\ 0 & 0 & 0 & \vdots & 0 & 0 & 1 & 0 & 0 & 0 & 0 & 0 & -1 \\ 0 & 0 & 0 & \vdots & 0 & 0 & 0 & 1 & 0 & 0 & -1 & 0 & 0 \\ 0 & 0 & 0 & \vdots & 0 & 0 & 0 & 0 & 1 & 0 & 0 & -1 & 0 \\ 0 & 0 & 0 & \vdots & 0 & 0 & 0 & 0 & 0 & 1 & 0 & 0 & -1 \end{bmatrix} \tag{13}$$

$$\begin{bmatrix} E_{1a} \\ E_{1b} \\ E_{1c} \\ E_{2a} \\ E_{2b} \\ E_{2c} \\ E_{3a} \\ E_{3b} \\ E_{3c} \\ E_{4a} \\ E_{4b} \\ E_{4c} \end{bmatrix} = \begin{bmatrix} 1 & 0 & 0 & -1 & 0 & 0 & 0 & 0 & 0 & 0 & 0 & 0 & 0 \\ 0 & 1 & 0 & 0 & -1 & 0 & 0 & 0 & 0 & 0 & 0 & 0 & 0 \\ 0 & 0 & 1 & 0 & 0 & -1 & 0 & 0 & 0 & 0 & 0 & 0 & 0 \\ 1 & 0 & 0 & 0 & 0 & 0 & -1 & 0 & 0 & 0 & 0 & 0 & 0 \\ 0 & 1 & 0 & 0 & 0 & 0 & 0 & -1 & 0 & 0 & 0 & 0 & 0 \\ 0 & 0 & 1 & 0 & 0 & 0 & 0 & 0 & -1 & 0 & 0 & 0 & 0 \\ 0 & 0 & 0 & 1 & 0 & 0 & 0 & 0 & 0 & -1 & 0 & 0 & 0 \\ 0 & 0 & 0 & 0 & 1 & 0 & 0 & 0 & 0 & 0 & -1 & 0 & 0 \\ 0 & 0 & 0 & 0 & 0 & 1 & 0 & 0 & 0 & 0 & 0 & -1 & 0 \\ 0 & 0 & 0 & 0 & 0 & 0 & 1 & 0 & 0 & -1 & 0 & 0 & 0 \\ 0 & 0 & 0 & 0 & 0 & 0 & 0 & 1 & 0 & 0 & -1 & 0 & 0 \\ 0 & 0 & 0 & 0 & 0 & 0 & 0 & 0 & 1 & 0 & 0 & 0 & -1 \end{bmatrix} \begin{bmatrix} V_{1a} \\ V_{1b} \\ V_{1c} \\ V_{2a} \\ V_{2b} \\ V_{2c} \\ V_{3a} \\ V_{3b} \\ V_{3c} \\ V_{4a} \\ V_{4b} \\ V_{4c} \end{bmatrix}, \tag{16}$$

$$\mathbf{I}_{3\phi} = \mathbf{A}_{3\phi}^T \mathbf{J}_{3\phi} \quad (21)$$

where $\mathbf{I}_{3\phi}$ represents the vector of net injected currents, and $\mathbf{J}_{3\phi}$ denotes the vector of the branch currents.

Since the substation currents (*i.e.*, I_{1a}, I_{1b}, I_{1c}) are unknown variables, which will depend on the final solution to the power flow problem, Equation (21) is only limited to the relationship between currents at the demand nodes and the branch currents, as defined in (22).

$$\mathbf{I}_{d3\phi} = \mathbf{A}_{d3\phi}^T \mathbf{J}_{3\phi} \quad (22)$$

In order to relate the voltage drops in the branches to their corresponding currents, the three-phase version of the branch impedance matrix $\mathbf{Z}_{L3\phi}$ is used. This matrix is defined in (23), and the relationship between voltages and currents is presented in (24).

$$\mathbf{E}_{L3\phi} = \mathbf{Z}_{L3\phi} \mathbf{J}_{3\phi} \quad (24)$$

Now, an equation is needed which relates the three-phase demand voltages to the three-phase demand currents. Therefore, the above-presented equations, such as (24), which uses the inverse of the impedance matrix $\mathbf{Z}_{3\phi}$ to

clear the currents in the lines $\mathbf{J}_{3\phi}$, are replaced into Equation (22) to obtain the following:

$$\mathbf{I}_{d3\phi} = \mathbf{A}_{d3\phi}^T \mathbf{Z}_{L3\phi}^{-1} \mathbf{E}_{L3\phi}, \quad (25)$$

Equation (18), which expresses the voltage drops in the lines, can be replaced into (25) as follows:

$$\mathbf{I}_{d3\phi} = \mathbf{A}_{d3\phi}^T \mathbf{Z}_{L3\phi}^{-1} \mathbf{A}_{s3\phi} \mathbf{V}_{s3\phi} + \mathbf{A}_{d3\phi}^T \mathbf{Z}_{L3\phi}^{-1} \mathbf{A}_{d3\phi} \mathbf{V}_{d3\phi} \quad (26)$$

$$\mathbf{I}_{d3\phi} = \mathbf{A}_{d3\phi}^T \mathbf{Y}_{L3\phi} \mathbf{A}_{s3\phi} \mathbf{V}_{s3\phi} + \mathbf{A}_{d3\phi}^T \mathbf{Y}_{L3\phi} \mathbf{A}_{d3\phi} \mathbf{V}_{d3\phi} \quad (27)$$

$$\mathbf{I}_{d3\phi} = \mathbf{Y}_{ds3\phi} \mathbf{V}_{s3\phi} + \mathbf{Y}_{dd3\phi} \mathbf{V}_{d3\phi} \quad (28)$$

In Equation (28), two new terms are evident, namely $\mathbf{Y}_{ds3\phi} = \mathbf{A}_{d3\phi}^T \mathbf{Y}_{L3\phi} \mathbf{A}_{s3\phi}$ and $\mathbf{Y}_{dd3\phi} = \mathbf{A}_{d3\phi}^T \mathbf{Y}_{L3\phi} \mathbf{A}_{d3\phi}$. From this equation, the three-phase voltages at the demand nodes are cleared to obtain the following:

where $\mathbf{V}_{s3\phi}$ is the vector of the voltages assigned to the substation, which, for the power flow problem, are assumed to be known [44].

$$\begin{bmatrix} I_{1a} \\ I_{1b} \\ I_{1c} \\ I_{2a} \\ I_{2b} \\ I_{2c} \\ I_{3a} \\ I_{3b} \\ I_{3c} \\ I_{4a} \\ I_{4b} \\ I_{4c} \end{bmatrix} = \begin{bmatrix} 1 & 0 & 0 & 1 & 0 & 0 & 0 & 0 & 0 & 0 & 0 \\ 0 & 1 & 0 & 0 & 1 & 0 & 0 & 0 & 0 & 0 & 0 \\ 0 & 0 & 1 & 0 & 0 & 1 & 0 & 0 & 0 & 0 & 0 \\ -1 & 0 & 0 & 0 & 0 & 0 & 1 & 0 & 0 & 0 & 0 \\ 0 & -1 & 0 & 0 & 0 & 0 & 0 & 1 & 0 & 0 & 0 \\ 0 & 0 & -1 & 0 & 0 & 0 & 0 & 0 & 1 & 0 & 0 \\ 0 & 0 & 0 & -1 & 0 & 0 & 0 & 0 & 0 & 1 & 0 \\ 0 & 0 & 0 & 0 & -1 & 0 & 0 & 0 & 0 & 0 & 1 \\ 0 & 0 & 0 & 0 & 0 & -1 & 0 & 0 & 0 & 0 & 0 \\ 0 & 0 & 0 & 0 & 0 & 0 & -1 & 0 & 0 & -1 & 0 \\ 0 & 0 & 0 & 0 & 0 & 0 & 0 & -1 & 0 & 0 & -1 \\ 0 & 0 & 0 & 0 & 0 & 0 & 0 & 0 & -1 & 0 & 0 \end{bmatrix} \begin{bmatrix} J_{1a} \\ J_{1b} \\ J_{1c} \\ J_{2a} \\ J_{2b} \\ J_{2c} \\ J_{3a} \\ J_{3b} \\ J_{3c} \\ J_{4a} \\ J_{4b} \\ J_{4c} \end{bmatrix} \quad (20)$$

$$\mathbf{Z}_{L3\phi} = \begin{bmatrix} Z_{1aa} & Z_{1ab} & Z_{1ac} & 0 & 0 & 0 & 0 & 0 & 0 & 0 & 0 \\ Z_{1ba} & Z_{1bb} & Z_{1bc} & 0 & 0 & 0 & 0 & 0 & 0 & 0 & 0 \\ Z_{1ca} & Z_{1cb} & Z_{1cc} & 0 & 0 & 0 & 0 & 0 & 0 & 0 & 0 \\ 0 & 0 & 0 & Z_{2aa} & Z_{2ab} & Z_{2ac} & 0 & 0 & 0 & 0 & 0 \\ 0 & 0 & 0 & Z_{2ba} & Z_{2bb} & Z_{2bc} & 0 & 0 & 0 & 0 & 0 \\ 0 & 0 & 0 & Z_{2ca} & Z_{2cb} & Z_{2cc} & 0 & 0 & 0 & 0 & 0 \\ 0 & 0 & 0 & 0 & 0 & 0 & Z_{3aa} & Z_{3ab} & Z_{3ac} & 0 & 0 \\ 0 & 0 & 0 & 0 & 0 & 0 & Z_{3ba} & Z_{3bb} & Z_{3bc} & 0 & 0 \\ 0 & 0 & 0 & 0 & 0 & 0 & Z_{3ca} & Z_{3cb} & Z_{3cc} & 0 & 0 \\ 0 & 0 & 0 & 0 & 0 & 0 & 0 & 0 & 0 & Z_{4aa} & Z_{4ab} & Z_{4ac} \\ 0 & 0 & 0 & 0 & 0 & 0 & 0 & 0 & 0 & Z_{4ba} & Z_{4bb} & Z_{4bc} \\ 0 & 0 & 0 & 0 & 0 & 0 & 0 & 0 & 0 & Z_{4ca} & Z_{4cb} & Z_{4cc} \end{bmatrix} \quad (23)$$

To find the three-phase voltages at the demand nodes in (29), the currents in the three-phase loads $I_{d3\phi}$ are needed. These currents depend on the connection of the loads, and they can have a Δ connection (Figure 3) or a Y connection (Figure 4), considering that m refers to the node number.

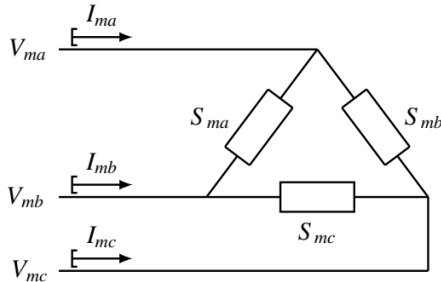


Figure 3. Δ connection

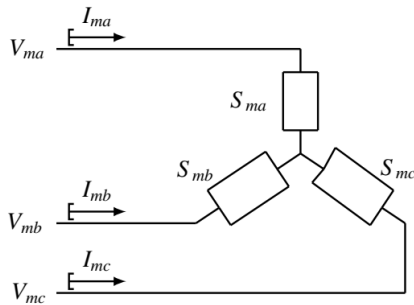


Figure 4. Y connection

Equations (30)–(32) derive the currents in the loads in triangle connection, and Equations (33)–(35) derive the

$$I_{ma} = \left(\frac{S_{ma}}{V_{ma} - V_{mb}} \right)^* - \left(\frac{S_{mc}}{V_{mc} - V_{ma}} \right)^* \quad (30)$$

$$I_{mb} = \left(\frac{S_{mb}}{V_{mb} - V_{mc}} \right)^* - \left(\frac{S_{ma}}{V_{ma} - V_{mb}} \right)^* \quad (31)$$

$$I_{mc} = \left(\frac{S_{mc}}{V_{mc} - V_{ma}} \right)^* - \left(\frac{S_{mb}}{V_{mb} - V_{mc}} \right)^* \quad (32)$$

$$I_{ma} = \left(\frac{S_{ma}}{V_{ma}} \right)^* \quad (33)$$

$$I_{mb} = \left(\frac{S_{mb}}{V_{mb}} \right)^* \quad (34)$$

$$I_{mc} = \left(\frac{S_{mc}}{V_{mc}} \right)^* \quad (35)$$

Finally, in order to obtain the solution of the power flow problem in (29), an iterative process c is employed until the desired convergence is reached (i.e., $|\mathbf{V}_{d3\phi}^{c+1} - \mathbf{V}_{d3\phi}^c| \leq \varepsilon$, where ε is the expected convergence error, which is assigned as 1×10^{-10}). The iterative form of (29) is shown in (36).

$$\mathbf{V}_{d3\phi}^{c+1} = -\mathbf{Y}_{dd3\phi}^{-1} (\mathbf{I}_{d3\phi}^c + \mathbf{Y}_{ds3\phi} \mathbf{V}_{s3\phi}) \quad (36)$$

Once the voltages of the demand nodes are known, the power losses of the demand node are obtained as follows:

$$P_{\text{loss}} = \text{real}\{\mathbf{E}_{L3\phi}^T \mathbf{I}_{3\phi}^*\} \quad (37)$$

Remark 3. The effect of each load configuration provided by the master stage is observed in the current calculation of each node, as seen in Equations (31)–(35), which implies that the slave stage, i.e., Equation (36), is the heart of the proposed optimization approach, as it is in charge of defining the power losses value for its solution individual in (7). Thus, it is entrusted with guiding the SSA during the exploration and exploitation of the solution space.

3.3. Summary of the optimization approach

Algorithm 1 shows the general implementation of the SSA. It starts by entering information to solve three-phase flows, such as the electrical parameters, the loads in each phase, and the connection of the nodes.

Data: Define the three-phase network under analysis
 Declare each one of the parameters of the SSA;
 Generate the initial population of salps using Equation (8);
 Evaluate the objective function with Equation (1) for each individual;
 Establish the best global individual (*BEST*) as the leader of the salp chain.

```

1 for  $t = 1 : t_{\text{máx}}$  do
2   for  $i = 1 : N_s$  do
3     Calculate the new position  $x_i^{t+1}$ ;
4     Check the limits of  $x_i^{t+1}$  as a possible
       solution;
5   for  $j = 1 : N_s$  do
6     Review the feasibility of new positions;
7     Determine whether the new salps string will
       replace  $x_i^t$ ;
8   Update the BEST solution to find a better
       individual;

```

Algoritmo 1. General implementation of the SSA in the master stage

The SSA's evolution criterion guarantees the search for new individuals and the convergence of the results. The initial population is generated, and the objective function of Equation (1) is used to establish the *BEST* solution. From this point, the evolution criteria are used to calculate the new position x_i^{t+1} , and the limits of the integer variables should correspond. The latest population is checked, which must have a lower value than the *BEST* individual for it to replace the previous solution group and continue the cycle until convergence is reached.

4. Characteristics of the three-phase asymmetric distribution grids

This section shows the characteristics of the three asymmetric networks used (*i.e.*, the three-phase systems with 8, 25, and 37 nodes). These are three typical networks used in the specialized literature to validate master-slave optimization methods with the aim of minimizing grid power losses via optimal load balancing

[33]. The main characteristics of these test feeders are listed below.

4.1. IEEE 8-bus grid

This 8-node IEEE asymmetrical distribution system has a radial configuration, one slack node, and seven demand nodes. It uses a nominal voltage of 11 kV [45] and has seven three-phase lines. Figure 5 shows the configuration of the 8-node system.

The parametric information regarding the load values per node and the branch parameters is listed in Tables 3 and 4.

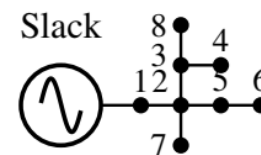


Figure 5. Electrical configuration of the 8-node threephase test system.

Table 3. Line and node parameters in the 8-node system

Line	Node i	Node j	Conductor	Length [ft]	P _{JA} (kW)	Q _{JA} (kvar)	P _{JB} (kW)	Q _{JB} (kvar)	P _{JC} (kW)	Q _{JC} (kvar)
1	1	2	1	5280	519	250	259	126	515	250
2	2	3	2	5280	0	0	259	126	486	235
3	2	5	3	5280	0	0	0	0	226	109
4	2	7	3	5280	486	235	0	0	0	0
5	3	4	4	5280	0	0	0	0	324	157
6	3	8	5	5280	0	0	267	129	0	0
7	5	6	6	5280	0	0	0	0	145	70

Table 4. Impedance matrix for conductor types in the 8-node system

Conductor	Impedance Matrix (Ω/mi)		
1	$0,093654 + j0,0402930$	$0,031218 + j0,0134310$	$0,031218 + j0,0134310$
	$0,031218 + j0,0134310$	$0,093654 + j0,0402930$	$0,031218 + j0,0134310$
	$0,031218 + j0,0134310$	$0,031218 + j0,0134310$	$0,093654 + j0,0402930$
2	$0,156090 + j0,0671550$	$0,052030 + j0,0223850$	$0,052030 + j0,0223850$
	$0,052030 + j0,0223850$	$0,156090 + j0,0671550$	$0,052030 + j0,0223850$
	$0,052030 + j0,0223850$	$0,052030 + j0,0223850$	$0,156090 + j0,0671550$
3	$0,046827 + j0,0201465$	$0,015609 + j0,0067155$	$0,015609 + j0,0067155$
	$0,015609 + j0,0067155$	$0,046827 + j0,0201465$	$0,015609 + j0,0067155$
	$0,015609 + j0,0067155$	$0,015609 + j0,0067155$	$0,046827 + j0,0201465$
4	$0,031218 + j0,0134310$	$0,010406 + j0,0044770$	$0,010406 + j0,0044770$
	$0,010406 + j0,0044770$	$0,031218 + j0,0134310$	$0,010406 + j0,0044770$
	$0,010406 + j0,0044770$	$0,010406 + j0,0044770$	$0,031218 + j0,0134310$
5	$0,062436 + j0,0268620$	$0,020812 + j0,0089540$	$0,020812 + j0,0089540$
	$0,020812 + j0,0089540$	$0,062436 + j0,0268620$	$0,020812 + j0,0089540$
	$0,020812 + j0,0089540$	$0,020812 + j0,0089540$	$0,062436 + j0,0268620$
6	$0,078045 + j0,0335775$	$0,026015 + j0,0111925$	$0,026015 + j0,0111925$
	$0,026015 + j0,0111925$	$0,078045 + j0,0335775$	$0,026015 + j0,0111925$
	$0,026015 + j0,0111925$	$0,026015 + j0,0111925$	$0,078045 + j0,0335775$

4.2. IEEE 25-bus grid

This asymmetrical 25-node IEEE test system has a radial configuration, in addition to one slack node, 22 demand nodes, 24 three-phase distribution lines, and a nominal voltage of 4.16 kV [46]. The configuration of this test system can be seen in Figure 6.

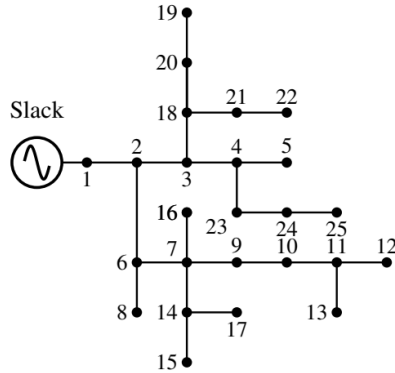


Figure 6. Electrical configuration of the IEEE 25-node three-phase test system.

The parametric information regarding the load values per node and the branch parameters is listed in Table 5 and Table 6.

4.3. IEEE 37-bus grid

This 37-node test system corresponds to a three-phase asymmetrical IEEE distribution network located in California, USA, with one slack node, 25 demand nodes, and 35 distribution lines, as well as a nominal voltage of 4.8 kV. This test network is an adaptation of the one stated in [47].

Its configuration is depicted in Figure 7. The parametric information regarding the load values per node and the branch parameters is listed in Tables 7 and 8.

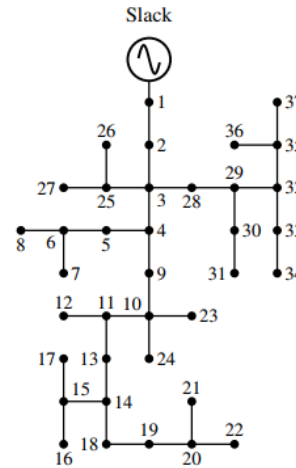


Figure 7. Electrical configuration of the IEEE 37-node three-phase test system.

Table 5. Line and node parameters in the 25-node system

Line	Node i	Node j	Conductor	Length [ft]	P_{jA} (kW)	Q_{jA} (kvar)	P_{jB} (kW)	Q_{jB} (kvar)	P_{jC} (kW)	Q_{jC} (kvar)
1	1	2	1	1000	0	0	0	0	0	0
2	2	3	1	500	36	21.6	28.8	19.2	42	26.4
3	2	6	2	500	43.2	28.8	33.6	24	30	30
4	3	4	1	500	57.6	43.2	4.8	3.4	48	30
5	3	18	2	500	57.6	43.2	38.4	28.8	48	36
6	4	5	2	500	43.2	28.8	28.8	19.2	36	24
7	4	23	2	400	8.6	64.8	4.8	3.8	60	42
8	6	7	2	500	0	0	0	0	0	0
9	6	8	2	1000	43.2	28.8	28.8	19.2	3.6	2.4
10	7	9	2	500	72	50.4	38.4	28.8	48	30
11	7	14	2	500	57.6	36	38.4	28.8	60	42
12	7	16	2	500	57.6	4.3	3.8	28.8	48	36
13	9	10	2	500	36	21.6	28.8	19.2	32	26.4
14	10	11	2	300	50.4	31.7	24	14.4	36	24
15	11	12	3	200	57.6	36	48	33.6	48	36
16	11	13	3	200	64.8	21.6	33.6	21.1	36	24
17	14	15	2	300	7.2	4.3	4.8	2.9	6	3.6
18	14	17	3	300	57.6	43.2	33.6	24	54	38.4
19	18	20	2	500	50.4	36	38.4	28.8	54	38.4
20	18	21	3	400	5.8	4.3	3.4	2.4	5.4	3.8
21	20	19	3	400	8.6	6.5	4.8	3.4	6	4.8
22	21	22	3	400	72	50.4	57.6	43.2	60	48
23	23	24	2	400	50.4	36	43.2	30.7	4.8	3.6
24	24	25	3	400	8.6	6.5	4.8	2.9	6	4.2

Table 6. Impedance matrix for conductor types in the 25-node system

Conductor	Impedance Matrix (Ω/mi)		
	1	$0,3686 + j0,6852$	$0,0169 + j0,1515$
	$0,0169 + j0,1515$	$0,3757 + j0,6715$	$0,0188 + j0,2072$
	$0,0155 + j0,1098$	$0,0188 + j0,2072$	$0,3723 + j0,6782$
2	$0,9775 + j0,8717$	$0,0167 + j0,1697$	$0,0152 + j0,1264$
	$0,0167 + j0,1697$	$0,9844 + j0,8654$	$0,0186 + j0,2275$
	$0,0152 + j0,1264$	$0,0186 + j0,2275$	$0,9810 + j0,8648$
3	$1,9280 + j1,4194$	$0,0161 + j0,1183$	$0,0161 + j0,1183$
	$0,0161 + j0,1183$	$1,9308 + j1,4215$	$0,0161 + j0,1183$
	$0,0161 + j0,1183$	$0,0161 + j0,1183$	$1,9337 + j1,4236$

Table 7. Line and node parameters in the 37-node system

Line	Node i	Node j	Conductor	Length [ft]	P_{jA} (kW)	Q_{jA} (kvar)	P_{jB} (kW)	Q_{jB} (kvar)	P_{jC} (kW)	Q_{jC} (kvar)
1	1	2	1	1850	140	70	140	70	350	175
2	2	3	2	960	0	0	0	0	0	0
3	3	24	4	400	0	0	0	0	0	0
4	3	27	3	360	0	0	0	0	85	40
5	3	4	2	1320	0	0	0	0	0	0
6	4	5	4	240	0	0	0	0	42	21
7	4	9	3	600	0	0	0	0	85	40
8	5	6	3	280	42	21	0	0	0	0
9	6	7	4	200	42	21	42	21	42	21
10	6	8	4	280	42	21	0	0	0	0
11	9	10	3	200	0	0	0	0	0	0
12	10	23	3	600	0	0	85	40	0	0
13	10	11	3	320	0	0	0	0	0	0
14	11	13	3	320	85	40	0	0	0	0
15	11	12	4	320	0	0	0	0	42	21
16	13	14	3	560	0	0	0	0	42	21
17	14	18	3	640	140	70	0	0	0	0
18	14	15	4	520	0	0	0	0	0	0
19	15	16	4	200	0	0	0	0	85	40
20	15	17	4	1280	0	0	42	21	0	0
21	18	19	3	400	126	62	0	0	0	0
22	19	20	3	400	0	0	0	0	0	0
23	20	22	3	400	0	0	0	0	42	21
24	20	21	4	200	0	0	0	0	85	40
25	24	26	4	320	8	4	85	40	0	0
26	24	25	4	240	0	0	0	0	85	40
27	27	28	3	520	0	0	0	0	0	0
28	28	29	4	80	17	8	21	10	0	0
29	28	31	3	800	0	0	0	0	85	40
30	29	30	4	520	85	40	0	0	0	0
31	31	34	4	920	0	0	0	0	0	0
32	31	32	3	600	0	0	0	0	0	0
33	32	33	4	280	0	0	42	21	0	0
34	34	36	4	760	0	0	42	21	0	0
35	34	35	4	120	0	0	140	70	21	10

5. Analysis of results and validation of the methodology

This section presents the results and subsequent numerical validations obtained from applying the master-slave optimization based on the combination of the SSA and the backward/forward matrix power flow approach

to solve the phase imbalance problem in the three test systems. All of the simulations in this report were performed on a computer with an Intel(R) Core (TM) i5-6198U 2.40 GHz processor, 8 GB RAM, a Windows 10 Home operating system, and the MATLAB 2022a software. Table 9 shows the initial losses per phase, as well as the total losses.

Table 8. Impedance matrix for conductor types in the 37-node system

Conductor	Impedance Matrix (Ω/mi)		
1	$0,2926 + j0,1973$	$0,0673 - j0,0368$	$0,0337 - j0,0417$
	$0,0673 - j0,0368$	$0,2646 + j0,1900$	$0,0673 - j0,0368$
	$0,0337 - j0,0417$	$0,0673 - j0,0368$	$0,2926 + j0,1973$
2	$0,4751 + j0,2973$	$0,1629 - j0,0326$	$0,1234 - j0,0607$
	$0,1629 - j0,0326$	$0,4488 + j0,2678$	$0,1629 - j0,0326$
	$0,1234 - j0,0607$	$0,1629 - j0,0326$	$0,4751 + j0,2973$
3	$1,2936 + j0,6713$	$0,4871 + j0,2111$	$0,4585 + j0,1521$
	$0,4871 + j0,2111$	$1,3022 + j0,6326$	$0,4871 + j0,2111$
	$0,4585 + j0,1521$	$0,4871 + j0,2111$	$1,2936 + j0,6713$
4	$2,0952 + j0,7758$	$0,5204 + j0,2738$	$0,4926 + j0,2123$
	$0,5204 + j0,2738$	$2,1068 + j0,7398$	$0,5204 + j0,2738$
	$0,4926 + j0,2123$	$0,5204 + j0,2738$	$2,0952 + j0,7758$

Table 9. Initial power active losses for each one of the test systems

Test system	Iterations	Processing time (s)	Phase A (kW)	Phase B (kW)	Phase C (kW)	Total losses (kW)
8	5	0.0905	1.7158	2.3305	9.9462	13.9925
25	9	0.1882	36.8801	14.7837	23.7570	75.4207
37	9	0.2919	27.1532	11.9143	37.0683	76.1357

In addition, the processing times and the number of iterations required to reach convergence were determined, observing that the processing time increased with the system size. These results are provided for each analysis case (8, 25, and 37 nodes) using the iterative sweep method as a three-phase power flow.

Remark 4. To determine the effectiveness of the matricial backward/forward power flow method in dealing with the power losses calculation for each test feeder, the DIGSILENT power systems software was used to validate the results via a three-phase unbalanced Newton- Raphson approach, as recommended by the authors of [33].

The SSA was parameterized to solve the studied problem for the analyzed test feeders, as presented in Table 10.

Table 10. Parameters used in the implementation of the SSA

SSA	
Number of candidate solutions	12
Number of iterations	1000
Generation of candidate solutions	Gaussian distribution
Three-phase power flow with iterative sweep	
Number of iterations	1000
Tolerance	1×10^{-10}
System test	
Number of evaluations	100

The parameters sought a balance in the number of candidate solutions and the number of iterations, given that altering one of these parameters could change the processing times and the overall solution. However, the time increases rapidly with the number of iterations, while the improvements in the objective functions are insignificant.

5.1. Numerical results for the IEEE 8-bus grid

Table 11 shows the results obtained by the proposed methodology in the 8-node distribution system. These results were compared with those of the reference case and other algorithms reported in the specialized literature with regard to the problem under study, namely the Chu & Beasley genetic algorithm (CBGA), the discrete vortex search algorithm (DVSA), and the improved crow search algorithm (ICSA). Note that all of these algorithms were used by the authors of [33] to solve the optimal phase-balancing problem in three-phase asymmetric networks.

Table 11 shows a significant reduction in the total active power losses; the losses obtained using the SSA change from 13.9925 kW in the base case to 10.5869 kW. However, compared to the other algorithms, there is no significant change in the reduction of losses. Each algorithm, including the SSA, converges to the same solution and reduces the total losses by about 24.33 %.

Table 11. Results of applying phase-balancing methods in the 8-node system

Method	Connections	Phase A (kW)	Phase B (kW)	Phase C (kW)	Total Losses (kW)
Benchmark Case	{ 1, 1, 1, 1, 1, 1, 1 }	1.7158	2.3305	9.9462	13.9925
CBGA	{ 6, 1, 5, 1, 4, 4, 1 }	2.7295	4.0957	3.7617	10.5869
DVSA	{ 6, 1, 5, 1, 2, 1, 1 }	2.7295	4.0957	3.7617	10.5869
ICSA	{ 2, 4, 5, 4, 6, 4, 3 }	2.7412	3.9930	3.8464	10.5869
SSA	{ 1, 6, 2, 1, 5, 3, 6 }	3.8464	2.7412	3.9993	10.5869

For the IEEE 8-bus grid, this is an expected behavior, given that the solution space is small (*i.e.*, 6^7 , which corresponds to 279936 possible solutions). This implies that any combinatorial optimization method can easily find the optimal solution. Nevertheless, this is not possible for a test feeder with a large number of nodes, since the solution space increases exponentially.

The significant differences between the algorithms lies in the type of connection with each demand node. This connection affects the power losses for each of the phases of the three-phase system and, therefore, the total losses (kW). The SSA achieves the worst results regarding the phase A and C active power losses than the other algorithms.

However, it achieves the best reduction in phase B. The implementation of the SSA shows an increase from 1.7158 to 3.8464 kW in active power in phase A, which represents an increase from 2.3305 to 2.7412 kW, and an important reduction from 9.9462 to 3.9993 kW with respect to the base case.

Figure 8 shows the change that occurs in the losses of each phase by applying phase-balancing via the SSA and, consequently, the total losses reduction compared to the base case.

5.2. Numerical results for the IEEE 25-bus grid

Table 12 presents a comparative analysis of the proposed SSA approach and the literature reports on solving the optimal phase-swapping problem for the IEEE 33-bus grid. The results show the corresponding connections at the demand nodes to achieve the stated active power losses per phase, as well as the total losses.

With respect to the IEEE 8-node three-phase system, there is a change in the results obtained after implementing the different methodologies, as the implementation of the algorithms does not converge to the same result (total active power losses).

The base case reports total losses of 75.4207 kW, and the CBGA, DVSA, and ICSA improve the base case results by 4.1484 and 4.1525 %. The SSA algorithm achieves better results than the other algorithms; it goes from a base case value of 75.4207 kW to 72.2865 kW, which constitutes a reduction of 4.1556 %. Figure 9 shows the significant change in phase and total losses with respect to the reference case as obtained by applying the SSA.

Note that the losses are divided into phases A, B, and C. In the case of phase A, there is a reduction from 36.8801 to 25.8208 kW, representing a 29.871 % reduction. However, the other algorithms achieve a better reduction in that phase. The proposed methodology provides a different result in phase B, as the active power losses increase from 14.7837 to 26.0953 kW with respect to the reference base case. Finally, in phase C, the SSA achieves the best losses reduction, *i.e.*, from 23.757kW in the base case to 20.3704 kW, which means 14.25 %.

5.3. Numerical results for the IEEE 25-bus grid

Table 13 presents the results obtained by implementing the proposed methodology in the IEEE 37-node distribution system.

Table 13 shows reductions in the total active power losses in each of the methods. In the case of the implemented SSA, they go from 76.1357 kW in the base case to 61.4797 kW. However, for this test system, the ICSA algorithm reports better results, with 61.4781 kW. The SSA algorithm shows a reduction of 19.25 % due to the connection changes in the different nodes of the system. By comparing the SSA with the ICSA, it can be seen that the losses in phases A and B are lower in the latter, and there are very similar losses between both phases in the former. In phase C, the losses are somewhat lower than in other algorithms.

Figure 10 depicts the active power losses in each of the phases and the total changes obtained via the SSA.

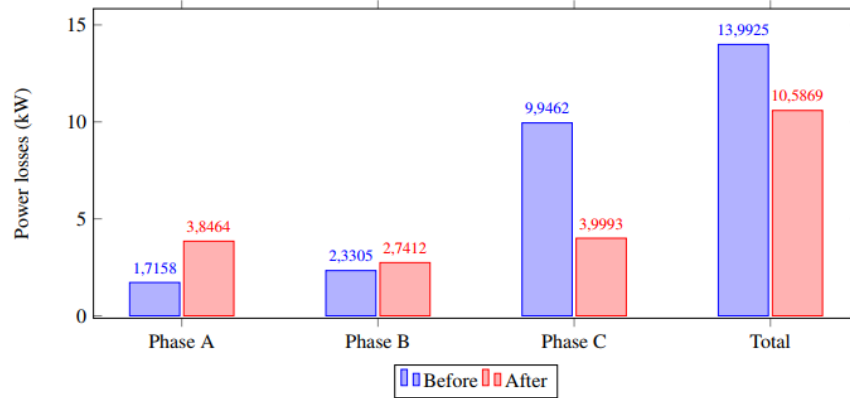


Figure 8. Phase balancing results obtained by implementing the SSA in the 8-node system.

Table 12. Results obtained by implementing the phase-balancing methods in the 25-node system

Method	Connections	Phase A (kW)	Phase B (kW)	Phase C (kW)	Total Losses (kW)
Benchmark Case	{1,1}	36.8801	14.7837	23.757	75.4207
CBGA	{1,1,3,5,2,1,1,1,2,6,5,1,5,3,6,6,3,3,1,3,5,2,4,3}	25.7626	25.9510	20.5782	72.2919
DVSA	{1,2,4,5,6,1,2,3,1,5,4,3,3,5,5,2,3,3,5,4,2,2,2,3}	25.6645	26.1613	20.4630	72.2888
ICSA	{4,2,4,5,6,3,2,3,1,5,4,3,3,5,5,2,3,3,5,4,2,2,2,3}	25.6645	26.1613	20.4630	72.2888
SSA	{3,6,3,2,6,4,4,6,1,5,4,3,3,5,5,2,3,6,1,3,5,5,3,4}	25.8208	26.0953	20.3704	72.2865

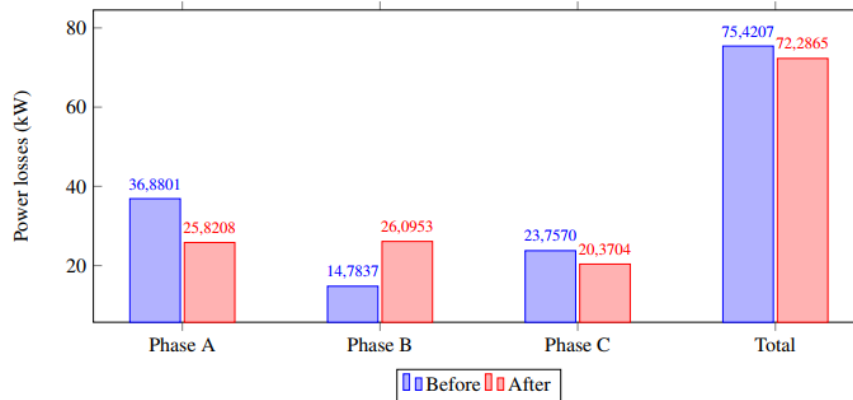


Figure 9. Phase-balancing results obtained by implementing the SSA in the 25-node system.

Table 13. Results obtained by applying phase-balancing methods to the 37-node system

Method	Connections	Phase A (kW)	Phase B (kW)	Phase C (kW)	Total Losses (kW)
Benchmark Case	{1,1}	36.8801	14.7837	23.757	75.4207
CBGA	{4,1,1,6,4,4,6,4,1,1,6,5,2,1,2,3,1,5,1,4,3,2,6,5,3,2,1,6,5,2,1,4,1,2,3}	25.7626	25.9510	20.5782	72.2919
DVSA	{4,1,1,5,3,4,2,3,1,1,3,2,2,1,3,5,2,3,1,3,6,1,2,3,3,2,1,1,2,4,1,4,1,2,4}	25.6645	26.1613	20.4630	72.2888
ICSA	{4,1,1,5,3,4,2,3,1,1,3,2,2,1,3,5,2,3,1,3,6,1,2,3,3,2,1,1,2,4,1,4,1,2,4}	25.6645	26.1613	20.4630	72.2888
SSA	{2,4,4,3,6,6,5,5,4,6,3,2,4,6,3,1,5,6,5,5,6,5,2,6,6,4,2,1,2,4,4,4,1,2,4}	25.8208	26.0953	20.3704	72.2865

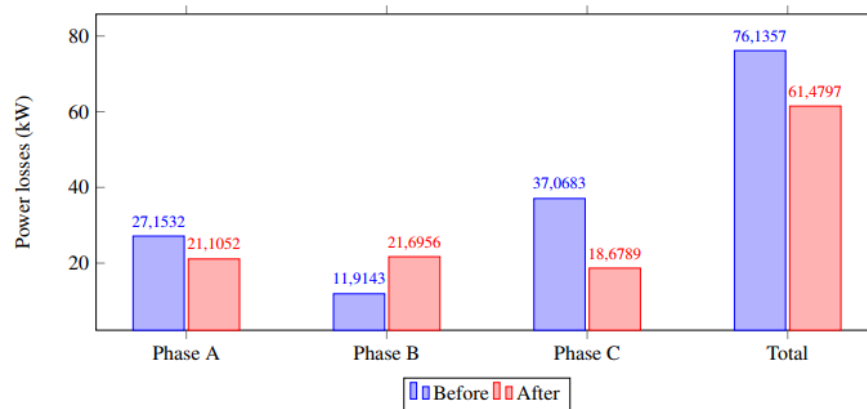


Figure 10. Phase-balancing results obtained by implementing the SSA in the 37-node system.

6. Conclusions and future works

This article addressed the optimal phase-balancing problem in three-phase asymmetric networks by applying a master-slave optimization methodology that combined the SSA approach in the master stage with the matricial backward/forward power flow method in the slave stage. The SSA approach was selected for the master stage due to its programming simplicity and its reportedly high efficiency in dealing with continuous and discrete optimization problems.

Numerical results in the IEEE 8-, 25-, and 37-node asymmetric distribution networks demonstrate the effectiveness of the SSA when compared to combinatorial optimizers (the Chu & Beasley genetic algorithm, the discrete vortex search algorithm, and the improved crow search algorithm).

As expected, the numerical results obtained for the IEEE 8-bus grid demonstrated that all of the analyzed combinatorial optimization methods – including the proposed solution methodology – provide the same numerical solution (perhaps the global optimum for this test feeder) due to the small size of its solution space (about 6^7), which is not the case for the IEEE 25- and 37-bus systems. For the latter, the proposed SSA approach reached the best numerical solution regarding the objective function value (*i.e.*, 72,2865 kW), which corresponds to a reduction of about 4,1556 % with respect to the bench- mark case, followed by the ICSA with a decrease of approximately 4,1525 %.

Nevertheless, in the IEEE 37-bus grid, the SSA approach was overcome by the ICSA, with a difference of 1,60 W, which allows stating that both optimization methodologies can be regarded as efficient in solving the optimal phase-balancing problem in three- phase asymmetric networks. Nevertheless, more research is

required for large-scale distribution grids in order to confirm this affirmation. The numerical results show a noticeable improvement obtained by applying the SSA to phase imbalances in the base cases of this study. However, the phase-balance problem has been addressed several times in the analyzed systems, and the differences between the results obtained by the SSA and those reported by other algorithms were not significant.

As future work, it will be possible to conduct the following studies:

- (i) applying emerging combinatorial optimization methodologies, such as the cat swarm optimization algorithm, the generalized normal distribution optimizer, and the locust search algorithm, among others;
- (ii) combining the phase-balancing problem with optimal reactive power compensation in order to reduce the expected annual costs of energy losses while including the investments required for capacitor banks; and
- (iii) performing a complete literature review of the existing methodologies for solving the phase-balancing problem in three-phase grids.

Autor Contributions

A. S. Vargas-Beltrán: Investigation, Conceptualization, Investigation, Methodology, Writing –original draft. O. M. Angarita-Santofimio: Conceptualization, Methodology, Writing –review& editing. O. D. Montoya: Supervision, Funding acquisition, Resources, Investigation, Conceptualization, Methodology, Writing –review& editing.

All authors have read and agreed to the published version of the manuscript.

Conflicts of Interest

The authors declare no conflict of interest.

Institutional Review Board Statement

Not applicable.

Informed Consent Statement

Not applicable.

References

- [1] W. A. Ñustes-Cuellar and S. R. Rivera-Rodriguez, "Colombia: Territorio de inversión en fuentes no convencionales de energía renovable para la generación eléctrica," in *Ingeniería Investigación y Desarrollo*, Jan. 2017, pp. 37–48, doi: <https://doi.org/10.19053/1900771X.v17.n1.2017.5954>
- [2] L. Berrio, C. Zuluaga, "Concepts, standards and communication technologies in smart grid," in *2012 IEEE 4th Colombian Workshop on Circuits and Systems (CWCAS)*, IEEE, Nov. 2012, pp. 1–6, doi: <https://doi.org/10.1109/CWCAS.2012.6404056>
- [3] L. F. Grisales Noreña, B. J. Restrepo Cuestas, F. E. Jaramillo Ramirez, "Ubicación y dimensionamiento de generación distribuida: Una revisión," *Cienc. e Ing. Neogranadina*, vol. 27, no. 2, pp. 157–176, Aug. 2017, doi: <https://doi.org/10.18359/rcin.2344>
- [4] F. M. Aboshady, D. W. P. Thomas, M. Sumner, "A Wideband Single End Fault Location Scheme for Active Untransposed Distribution Systems," *IEEE Trans. Smart Grid*, vol. 11, no. 3, pp. 2115–2124, 2020, doi: <https://doi.org/10.1109/TSG.2019.2947870>
- [5] S. D. Saldarriaga-Zuluaga, J. M. Lopez-Lezama, N. Munoz-Galeano, "Protection Coordination in Microgrids: Current Weaknesses, Available Solutions and Future Challenges," *IEEE Lat. Am. Trans.*, vol. 18, no. 10, pp. 1715–1723, Oct. 2020, doi: <https://doi.org/10.1109/TLA.2020.9387642>
- [6] A. Paz-Rodríguez, J. F. Castro-Ordoñez, O. D. Montoya, D. A. Giral-Ramírez, "Optimal Integration of Photovoltaic Sources in Distribution Networks for Daily Energy Losses Minimization Using the Vortex Search Algorithm," *Appl. Sci.*, vol. 11, no. 10, p. 4418, May 2021, doi: <https://doi.org/10.3390/app11104418>
- [7] S. Sultana, P. K. Roy, "Krill herd algorithm for optimal location of distributed generator in radial distribution system," *Appl. Soft Comput.*, vol. 40, pp. 391–404, Mar. 2016, doi: <https://doi.org/10.1016/j.asoc.2015.11.036>
- [8] S. Sultana, P. K. Roy, "Krill herd algorithm for optimal location of distributed generator in radial distribution system," *Appl. Soft Comput.*, vol. 40, no. 43, pp. 391–404, Mar. 2016, doi: <https://doi.org/10.1016/j.asoc.2015.11.036>
- [9] Z. Ullah, M. R. Elkadeem, S. Wang, J. Radosavljevic, "A Novel PSOS-CGSA Method for State Estimation in Unbalanced DG-Integrated Distribution Systems," *IEEE Access*, vol. 8, pp. 113219–113229, 2020, doi: <https://doi.org/10.1109/ACCESS.2020.3003521>
- [10] F. H. M. Rafi, M. J. Hossain, M. S. Rahman, S. Taghizadeh, "An overview of unbalance compensation techniques using power electronic converters for active distribution systems with renewable generation," *Renew. Sustain. Energy Rev.*, vol. 125, p. 109812, 2020, doi: <https://doi.org/10.1016/j.rser.2020.109812>
- [11] S. Sun, B. Liang, M. Dong, J. A. Taylor, "Phase Balancing Using Energy Storage in Power Grids Under Uncertainty," *IEEE Trans. Power Syst.*, vol. 31, no. 5, pp. 3891–3903, Sep. 2016, doi: <https://doi.org/10.1109/TPWRS.2015.2492359>
- [12] O. D. Montoya, L. F. Grisales-Noreña, E. Rivas-Trujillo, "Approximated Mixed-Integer Convex Model for Phase Balancing in Three-Phase Electric Networks," *Computers*, vol. 10, no. 9, p. 109, 2021, doi: <https://doi.org/10.3390/computers10090109>
- [13] C. A. Duarte Gualdrón, J. Bautista, G. Ordóñez, J. Barrero Perez, G. E. González Sua, "Medición de las magnitudes de potencia y energía eléctrica bajo las nuevas condiciones de los sistemas eléctricos," *Rev. UIS Ing.*, vol. 8, no. 1, pp. 9–19, 2009.
- [14] U. D. Lubo, "Cargos de respaldo por uso de la red eléctrica en el costo unitario de energía distribuida: desafíos y oportunidades para la planificación," *Rev. UIS Ing.*, vol. 18, no. 3, pp. 67–74, Apr. 2019, doi: <https://doi.org/10.18273/revuin.v18n3-2019007>

- [15] O. D. Montoya, A. Molina-Cabrera, L. F. Grisales-Noreña, R. A. Hincapié, M. Granada, “Improved Genetic Algorithm for Phase-Balancing in Three-Phase Distribution Networks: A Master-Slave Optimization Approach,” *Computation*, vol. 9, no. 6, p. 67, 2021, doi: <https://doi.org/10.3390/computation9060067>
- [16] G. Carrillo, J. F. Petit Suárez, “Reducción de pérdidas de potencia activa y mejoramiento de la calidad de la onda de tensión en sistemas de distribución,” *Rev. UIS Ing*, vol. 1, no. 1, pp. 59–66, 2002.
- [17] J. Zhu, G. Bilbro, Mo-Yuen Chow, “Phase balancing using simulated annealing,” *IEEE Trans. Power Syst.*, vol. 14, no. 4, pp. 1508–1513, 1999, doi: <https://doi.org/10.1109/59.801943>
- [18] M. A. Rios, J. C. Castano, A. Garces, and A. Molina-Cabrera, “Phase Balancing in Power Distribution Systems: A heuristic approach based on group-theory,” in *2019 IEEE Milan PowerTech, IEEE*, Jun. 2019, pp. 1–6. doi: <https://doi.org/10.1109/PTC.2019.8810723>
- [19] H. Khodr, I. Zerpa, P. De Oliveira-de Jesu’s, M. Matos, “Optimal Phase Balancing in Distribution System Using Mixed-Integer Linear Programming,” in *2006 IEEE/PES Transmission & Distribution Conference and Exposition: Latin America, IEEE*, 2006, pp. 1–5. doi: <https://doi.org/10.1109/TDCLA.2006.311368>
- [20] Bo Yang, Yunping Chen, Zunlian Zhao, Qiye Han, “A Master-Slave Particle Swarm Optimization Algorithm for Solving Constrained Optimization Problems,” in *2006 6th World Congress on Intelligent Control and Automation, IEEE*, 2006, pp. 3208–3212. doi: <https://doi.org/10.1109/WCICA.2006.1712959>
- [21] J. Zhu, C. Mo-Yuen, F. Zhang, “Phase balancing using mixed-integer programming [distribution feeders],” *IEEE Trans. Power Syst.*, vol. 13, no. 4, pp. 1487–1492, 1998, doi: <https://doi.org/10.1109/59.736295>
- [22] A. Correa, “Balance de fases multiobjetivo en sistemas de distribución,” *Sci. Tech.* Año XIII, vol. 37, no. 37, pp. 55–60, 2007.
- [23] A. Garcés Ruiz, M. Granada Echeverri, R. A. Gallego-R., “Balance de fases usando colonia de hormigas,” *Ing. Y Compet.*, vol. 7, no. 2, pp. 43–52, 2011, doi: <https://doi.org/10.25100/iyv.v7i2.2517>
- [24] A. G. Ruiz, J. C. G. Manso, R. A. Gallego Rendón, “Solución al problema de balance de fases y reconfiguración de alimentadores primarios bajo un modelamiento trifásico usando Simulated Annealing,” *Sci. Tech.* no. 30, pp. 37–42, 2006.
- [25] F. Postigo, et al. “Phase-selection algorithms to minimize cost and imbalance in U.S. synthetic distribution systems” *International Journal of Electrical Power & Energy Systems*, <https://doi.org/10.1016/j.ijepes.2020.106042>
- [26] G. A. Schweickardt G. Wiman, “Metaheurística Fepso multiobjetivo. Una aplicación para el análisis del balance de cargas en redes de distribución de baja tensión,” *Energética*, no. 41, pp. 33–48, 2008.
- [27] M. Sathiskumar, A. Nirmal kumar, L. Lakshminarasimman, S. Thiruvendakam, “A self adaptive hybrid differential evolution algorithm for phase balancing of unbalanced distribution system,” *Int. J. Electr. Power Energy Syst.*, vol. 42, no. 1, pp. 91–97, Nov. 2012, doi: <https://doi.org/10.1016/j.ijepes.2012.03.029>
- [28] R. Hooshmand, S. H. Soltani, “Simultaneous optimization of phase balancing and reconfiguration in distribution networks using BF–NM algorithm,” *Int. J. Electr. Power Energy Syst.*, vol. 41, no. 1, pp. 76–86, Oct. 2012, doi: <https://doi.org/10.1016/j.ijepes.2012.03.010>
- [29] P. Samal, S. Ganguly, S. Mohanty, “Planning of unbalanced radial distribution systems using differential evolution algorithm,” *Energy Syst.*, vol. 8, no. 2, pp. 389–410, 2017, doi: <https://doi.org/10.1007/s12667-016-0202-z>
- [30] I. P. Abril, “Multi-objective optimization of the balancing of phases in primary distribution circuits,” *Int. J. Electr. Power Energy Syst.*, vol. 82, pp. 420–428, 2016, doi: <https://doi.org/10.1016/j.ijepes.2016.03.047>
- [31] B. Cortés-Caicedo, L. S. Avellaneda-Gómez, O. D. Montoya, L. Alvarado-Barrios, H. R. Chamorro, “Application of the Vortex Search Algorithm to the Phase-Balancing Problem in Distribution Systems,” *Energies*, vol. 14, no. 5, p. 1282, 2021, doi: <https://doi.org/10.3390/en14051282>

- [32] H. Faris, S. Mirjalili, I. Aljarah, M. Mafarja, A. A. Heidari, “Salp Swarm Algorithm: Theory, Literature Review, and Application in Extreme Learning Machines,” in *Nature-Inspired Optimizers, in Studies in Computational Intelligence*. Cham: Springer International Publishing, 2020, pp. 185–199. doi: https://doi.org/10.1007/978-3-030-12127-3_11
- [33] B. Cortés-Caicedo, L. S. Avellaneda-Gómez, O. D. Montoya, L. Alvarado-Barrios, C. Álvarez-Arroyo, “An Improved Crow Search Algorithm Applied to the Phase Swapping Problem in Asymmetric Distribution Systems,” *Symmetry (Basel)*, vol. 13, no. 8, p. 1329, Jul. 2021, doi: <https://doi.org/10.3390/sym13081329>
- [34] V. C. Strezoski, L. D. Trpezanovski, “Three-phase asymmetrical load-flow,” *Int. J. Electr. Power Energy Syst.*, vol. 22, no. 7, pp. 511–520, Oct. 2000, doi: [https://doi.org/10.1016/S0142-0615\(00\)00012-0](https://doi.org/10.1016/S0142-0615(00)00012-0)
- [35] M. Granada Echeverri, R. A. Gallego Rendón, and J. M. López Lezama, “Planeamiento Óptimo de Balance de Fases para Reducción de Pérdidas en Sistemas de Distribución usando un Algoritmo Genético Especializado,” *Ing. y Cienc.*, vol. 8, no. 15, pp. 121–140, 2012.
- [36] L. Abualigah, M. Shehab, M. Alshinwan, H. Alabool, “Salp swarm algorithm: a comprehensive survey,” *Neural Comput. Appl.*, vol. 32, no. 15, pp. 11195–11215, Aug. 2020, doi: <https://doi.org/10.1007/s00521-019-04629-4>
- [37] S. Mirjalili, A. H. Gandomi, S. Z. Mirjalili, S. Saremi, H. Faris, S. M. Mirjalili, “Salp Swarm Algorithm: A bio-inspired optimizer for engineering design problems,” *Adv. Eng. Softw.*, vol. 114, pp. 163–191, Dec. 2017, doi: <https://doi.org/10.1016/j.advengsoft.2017.07.002>
- [38] L. S. Avellaneda-Gómez and O. D. Montoya-Giraldo, “Aplicación del algoritmo de optimización por enjambre de salpas para la estimación de parámetros en transformadores monofásicos empleando medidas de tensión y corriente,” *Rev. UIS Ing.*, vol. 21, no. 2, pp. 131–146, May 2022, doi: <https://doi.org/10.18273/revuin.v21n2-2022011>
- [39] S. Ben Chaabane, A. Belazi, S. Kharbech, A. Bouallegue, L. Clavier, “Improved Salp Swarm Optimization Algorithm: Application in Feature Weighting for Blind Modulation Identification,” *Electronics*, vol. 10, no. 16, p. 2002, 2021, doi: <https://doi.org/10.3390/electronics10162002>
- [40] R. A. Ibrahim, A. A. Ewees, D. Oliva, M. Abd Elaziz, S. Lu, “Improved salp swarm algorithm based on particle swarm optimization for feature selection,” *J. Ambient Intell. Humaniz. Comput.*, vol. 10, no. 8, pp. 3155–3169, Aug. 2019, doi: <https://doi.org/10.1007/s12652-018-1031-9>
- [41] H. Faris et al., “An efficient binary Salp Swarm Algorithm with crossover scheme for feature selection problems,” *Knowledge-Based Syst.*, vol. 154, pp. 43–67, Aug. 2018, doi: <https://doi.org/10.1016/j.knosys.2018.05.009>
- [42] H. Zhang et al., “A multi-strategy enhanced salp swarm algorithm for global optimization,” *Eng. Comput.*, vol. 38, no. 2, pp. 1177–1203, Apr. 2022, doi: <https://doi.org/10.1007/s00366-020-01099-4>
- [43] D. Shirmohammadi, H. W. Hong, A. Semlyen, G. X. Luo, “A compensation-based power flow method for weakly meshed distribution and transmission networks,” *IEEE Trans. Power Syst.*, vol. 3, no. 2, pp. 753–762, May 1988, doi: <https://doi.org/10.1109/59.192932>
- [44] T. Shen, Y. Li, J. Xiang, “A Graph-Based Power Flow Method for Balanced Distribution Systems,” *Energies*, vol. 11, no. 3, p. 511, Feb. 2018, doi: <https://doi.org/10.3390/en11030511>
- [45] R. P. Broadwater, A. Chandrasekaran, C. T. Huddleston, A. H. Khan, “Power flow analysis of unbalanced multiphase radial distribution systems,” *Electr. Power Syst. Res.*, vol. 14, no. 1, pp. 23–33, Feb. 1988, doi: [10.1016/0378-7796\(88\)90044-2](https://doi.org/10.1016/0378-7796(88)90044-2)
- [46] T. Ramana, V. Ganesh, S. Sivanagaraju, “Distributed Generator Placement And Sizing in Unbalanced Radial Distribution System,” *Cogener. Distrib. Gener. J.*, vol. 25, no. 1, pp. 52–71, Jan. 2010, doi: <https://doi.org/10.1080/15453661009709862>
- [47] W. H. Kersting, “Radial distribution test feeders,” *IEEE Trans. Power Syst.*, vol. 6, no. 3, pp. 975–985, 1991, doi: <https://doi.org/10.1109/59.119237>